Advanced HDPE with increased stiffness used for water supply networks

M. L. SCUTARU, H. TEODORESCU-DRAGHICESCU, S. VLASE*, M. MARIN
Transilvania University of Brasov, Department of Mechanical Engineering, 29 Eroilor Blvd, 500036, Brasov, Romania,

To increase the overall stiffness of a composite laminate is usual to use a polyester mat embedded as core in thin structures. This procedure can increase the structure's stiffness without increasing the thickness of a laminate.The paper presents the most important results obtained during three and four-point bend tests carried out on 20 × 2 mm, 25 × 2 mm, 40 × 2.3 mm, 63 × 4 mm and 90 × 6 mm high-density polyethylene (HDPE) pipelines used for water supply networks. In three-point bend tests the Young's modulus of bending decreases with the increase of pipelines' diameter. Main mechanical properties such Young's moduli of bending, flexural rigidity, stiffness, load/deflection at maximum deflection and load have been determined.

(Received July 2, 2014; accepted March 19, 2015)

Keywords: Overall stiffness, Composite laminate, High-density polyethylene, Stiffness, Water supply pipelines

1. Introduction

High-density polyethylene (HDPE) represents a thermoplastic material, which is suitable for manufacturing pipelines for water supply network applications. This material presents large strain values in tensile tests. High-density polyethylene can be reinforced with either glass or carbon fibers [1], [2]. To increase the overall stiffness of a composite laminate is usual to use a polyester mat embedded as core in thin structures. This procedure can increase the structure's stiffness without increasing the thickness of a laminate [8]. In general, in case of polymer matrix composites with three-phases, the elastic properties are quite difficult to predict.

Some authors tried to predict these elastic properties using some homogenization and averaging methods determining upper and lower limits of these properties [3]. To determine the stiffness of a material, the tensile test represents the basic static procedure to obtain the Young's modulus of any kind of material. Not only tensile tests but also static cyclic tension-compression tests have been used to determine important mechanical properties of composite laminates [4]. This procedure has been applied to three-phase polymer matrix composites also, using various load limits, number of cycles and test speeds [5]. If a fibers-reinforced composite laminate is subjected on directions that differ from the laminate's fibers directions then the stiffness may vary in quite large domains.

Young's moduli, shear moduli and Poisson ratios have been computed for various fibers-reinforced composite laminates subjected to off-axis loading systems. Some of these laminates present equal stiffness in all fibers disposal angles [6]. Theoretical approaches using the finite element method have been carried out for various fibers-reinforced composites as well as various laminates subjected to bending loads for mechanical characterization [7,8]. Some mechanical properties of advanced materials used in automotive engineering are presented in papers [9-12].

2. Theoretical approach

Since many pipelines used in wide range of applications include sandwich structures, a theoretical approach regarding these composite structures has been carried out below. The sandwich surface is different from the conventional laminates due to the core's characteristics. This core has to distance, support and bear the upper and lower skins and take only loads acting perpendicular to its surface. If the layers are relatively thin, the description of stress state and elements' stiffness is simplified, the base analysis of the sandwich behavior being the shell sandwich theory [16]. The strength of an ordinary sandwich element is determined by the bearing capability of its components. Thus, the core's loading capability is tested in shear and compression loadings. By peeling, the bond strength between core and skins is tested. A cross-section through a sandwich composite element is considered, consisting of three layers (two orthotropic skins and an isotropic core). This sandwich element is subjected to a tensile force n_x and to a bending moment m_x. The distribution of the normal stresses in case of a core with longitudinal stiffness is presented in figs. 1 and 2. In case of a core with longitudinal tensile stiffness, this feature can be computed using the skins and core Young's moduli as well as the skin's thickness (t) and core's height (h) [16]:

$$R_l = \frac{n_{xx}}{\varepsilon_{xx}} = \frac{\left(2t\sigma_{skin} + h\sigma_{core}\right)}{\varepsilon_{xx}} = 2E_{skin}\cdot t + E_{core}\cdot h\,. \quad (1)$$

The flexural rigidity can be computed using the same elements as well as the distance (a) between skins' median surfaces [16]:

$$R_i = \frac{m_x}{\kappa_x} = E_{skin}\cdot\left(\frac{t\,a^2}{2} + \frac{t^3}{6}\right) + \frac{E_{core}\cdot h^3}{12}\,, \quad (2)$$

where κ_x represents the curvature of the sandwich element on x-axis direction. In case of a core without longitudinal tensile stiffness, the skins and core stresses as well as the

resultant moments are presented in fig. 3. The forces in *x-y* plane are [13]:

$$\begin{bmatrix} n_{xx} \\ n_{yy} \\ n_{xy} \end{bmatrix} = n = n_1 + n_2 . \tag{3}$$

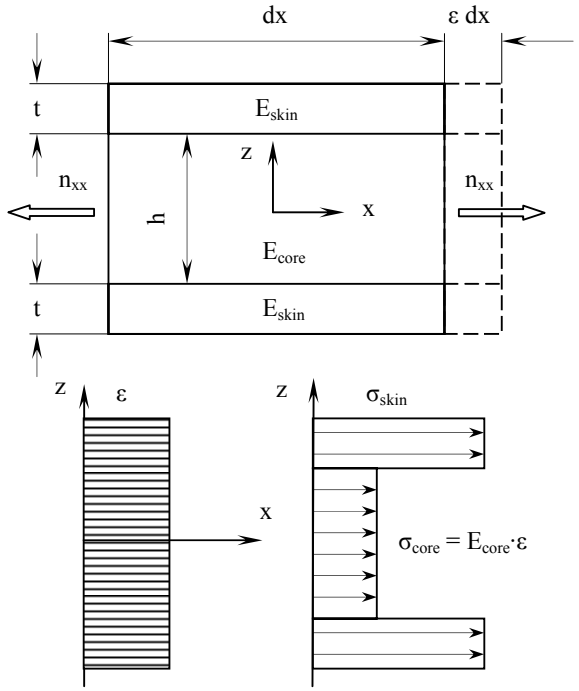

Fig. 1. Distribution of normal stresses in a sandwich element with core's longitudinal stiffness subjected to tensile loads [16]

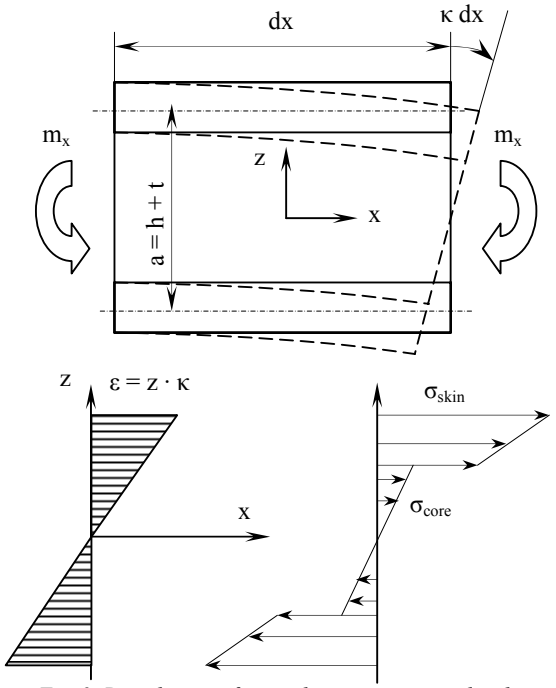

Fig. 2. Distribution of normal stresses in a sandwich element with core's longitudinal stiffness subjected to bending loads [16]

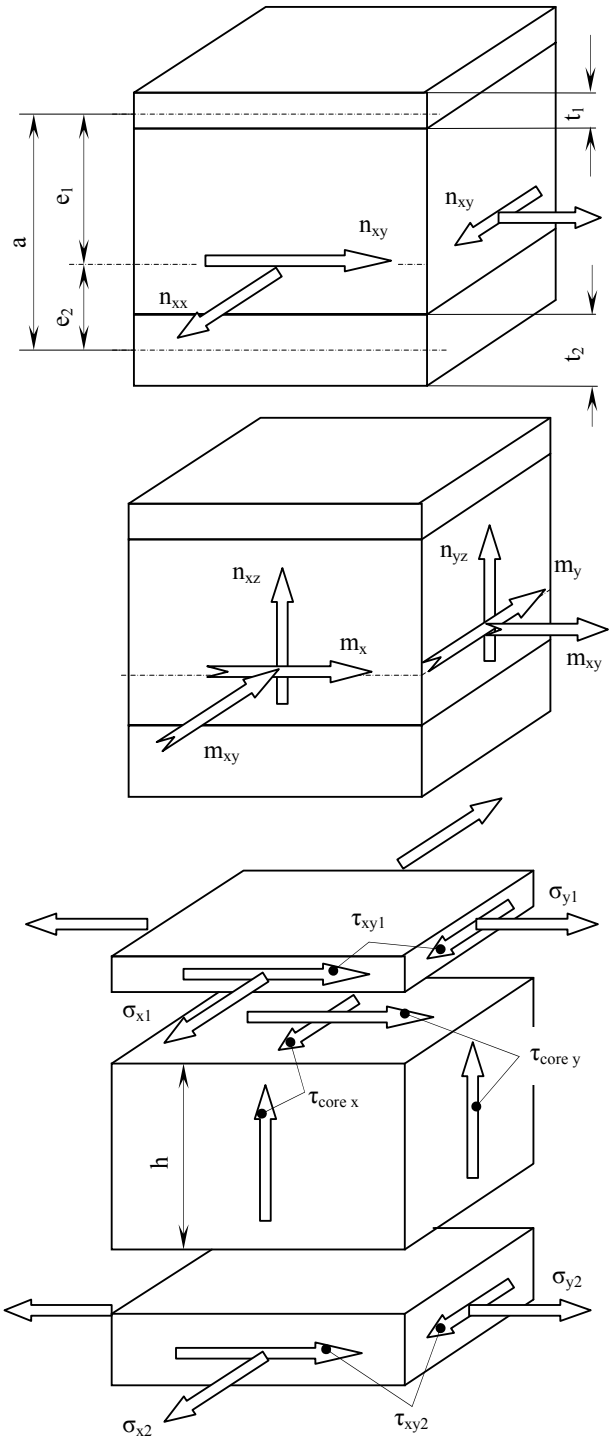

Fig. 3. Loads, moments and stresses in a sandwich with core without longitudinal stiffness [16]

The moments are [16]:

$$\begin{bmatrix} m_x \\ m_y \\ m_{xy} \end{bmatrix} = m = n_1 \cdot e_1 - n_2 \cdot e_2 . \tag{4}$$

The stresses are expressed in the following way [16]:

$$\sigma_1 \cdot t_1 = n_1 = \frac{n}{1+\frac{t_2}{t_1}} + \frac{m}{a}; \quad \sigma_2 \cdot t_2 = n_2 = \frac{n}{1+\frac{t_1}{t_2}} - \frac{m}{a}, \tag{5}$$

$$\tau_{core\,x} = \frac{n_{xz}}{a}; \quad \tau_{core\,y} = \frac{n_{yz}}{a}, \tag{6}$$

where:

$$a = h + \frac{t_1 + t_2}{2}. \tag{7}$$

The shear stresses distribution due to the action of transverse load is presented in Fig. 4.

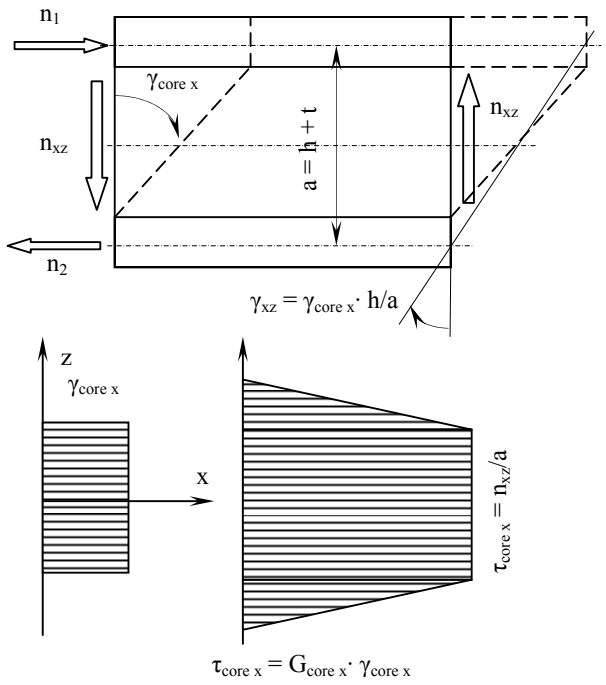

Fig. 4. Shear stresses distribution due to the action of n_{xz} transverse load [16]

Considering the core being isotropic, the γ_{xz} strain of the transverse cross-section is less than the $\gamma_{core\ x}$ strain, with the ratio h/a. The link between this strain and the n_{xz} transverse load is described by the shear stiffness M_x [16]:

$$M_x = \frac{n_{xz}}{\gamma_{xz}} = \frac{n_{xz} \cdot a}{\gamma_{core\ x} \cdot h} = G_{core\ x} \cdot \frac{a^2}{h} \approx G_{core\ x} \cdot a. \tag{8}$$

3. Material and method

In the Laboratory for Materials Testing, Department of Mechanical Engineering within Transilvania University of Brasov, Romania, both three-point as well as four-point bend tests have been carried out both on high-density polyethylene and on various pipelines with different diameters. The bend tests have been accomplished on LR5KPlus materials testing machine from Lloyd Instruments with following specifications:

- force range: up to 5 kN;
- load resolution: < 0.01% of load cell used;
- extension resolution: < 0.1 microns;
- load cell: XLC-5K-A1;
- analysis software: NEXYGEN Plus.

From 20 × 2 mm, 25 × 2 mm, 40 × 2.3 mm, 63 × 4 mm and 90 × 6 mm high-density polyethylene (HDPE) pipelines, specimens have been cut and subjected to four-point bend tests. These pipelines have been subjected to three-point bend tests also. Some four-point bend test features and specimens dimensions are presented in table 1.

Table 1. Specimens and four-point bend test features

Feature	Value
Gauge length (mm)	150
Test speed (mm/min)	20
Specimens width (mm)	10
Specimens thickness (mm)	4
Upper span (mm)	27
Lower span (mm)	80

4. Experimental results

Young's modulus of bending and load-deflection distributions of high-density polyethylene pipelines with following dimensions: 20 × 2 mm, 63 × 4 mm and 90 × 6 mm are presented in figs. 5-8.

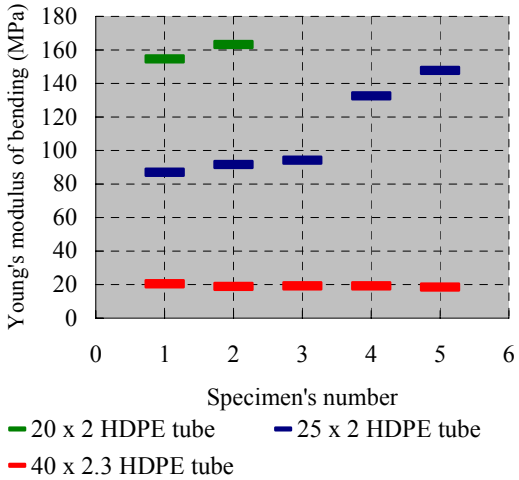

Fig. 5. Young's modulus of bending distributions of HDPE 20 x 2 mm, 25 x 2 mm and 40 x 2.3 mm pipelines

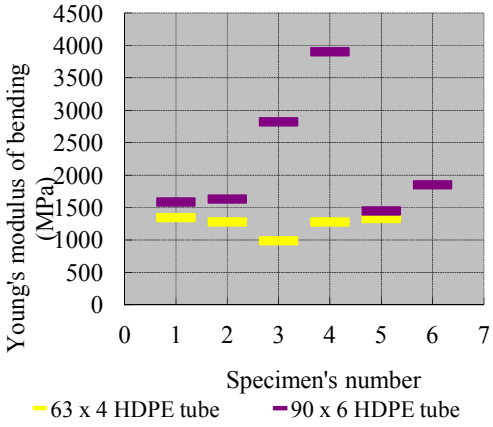

Fig. 6. Young's modulus of bending distributions of HDPE 63 × 4 mm and 90 × 6 mm pipelines

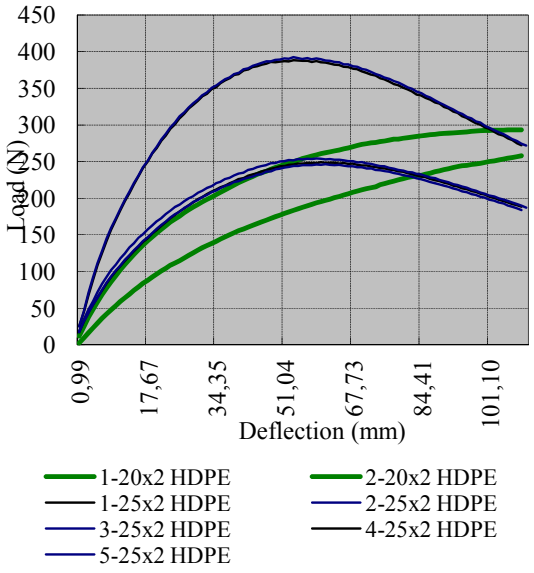

Fig. 7. Load-deflection distributions of HDPE 20 × 2 mm and 25 × 2 mm pipelines in three-point bend tests

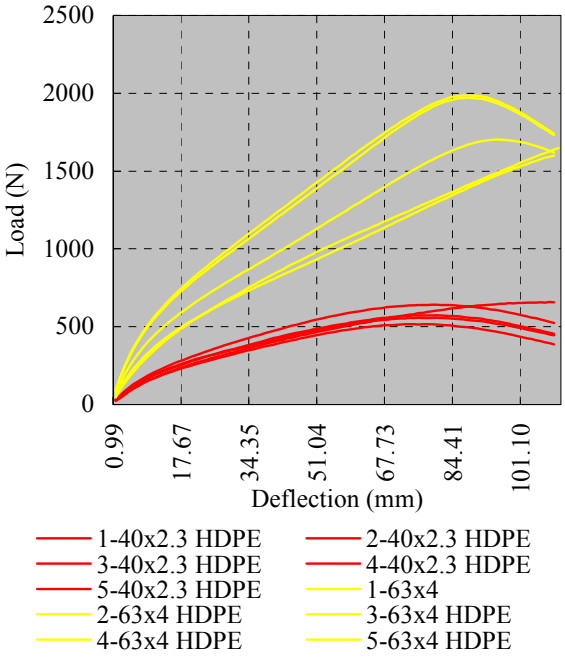

Fig. 8. Load-deflection distributions of HDPE 40 × 2.3 mm and 63 × 4 mm pipelines in three-point bend tests

5. Discussion and conclusions

The Young's modulus of bending distributions of high-density polyethylene 20 × 2 mm, 25 × 2 mm and 40 × 2.3 mm pipelines are ten times lower than the Young's modulus of bending distributions of high-density polyethylene 63 × 4 mm and 90 × 6 mm pipelines. The load-deflection distributions of high-density polyethylene 40 × 2.3 mm and 63 × 4 mm pipelines subjected to three-point bend tests are five times grater than the load-deflection distributions of high-density polyethylene 20 × 2 mm and 25 × 2 mm pipelines. Load-deflection distributions of HDPE specimens cut from 40 × 2.3 mm, 63 × 4 mm and 90 × 6 mm pipelines in four-point bend tests at 20 mm/min test speed are presented in fig. 9. In four-point bend tests, the bending between the upper span is considered more accurate than the bending in three-point bend test.

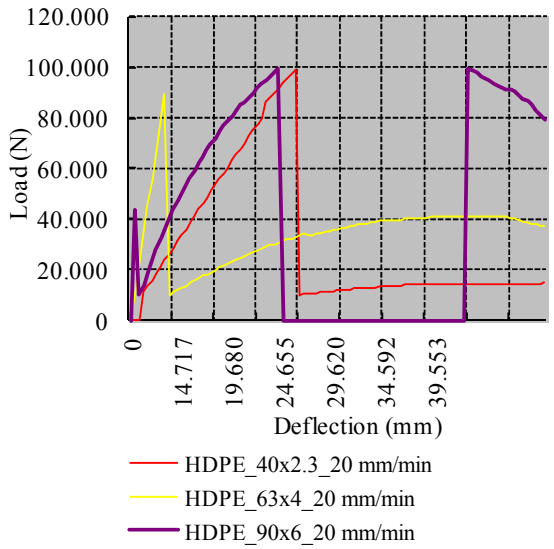

Fig. 9. Load-deflection distributions of HDPE specimens cut from 40 × 2.3 mm, 63 × 4 mm and 90 × 6 mm pipelines in four-point bend tests at 20 mm/min test speed

In case of three-point bend tests, with the increase of pipeline's diameter, the Young's modulus of bending decreases and the load-deflection distributions increase. The results show that this high-density polyethylene represents a suitable material to manufacture HDPE pipelines for water supply networks applications.

References

[1] N.D. Cristescu, E.M. Craciun, E. Soos, Mechanics of elastic composites, Chapman & Hall/CRC, (2003).
[2] H. Schürmann, Konstruiren mit Faser-Kunststoff-Verbunden, Springer, (2005).
[3] H. Teodorescu-Draghicescu, S. Vlase, Computational Materials Science, **50**(4), February (2011).
[4] H. Teodorescu-Draghicescu, S. Vlase, L. Scutaru, L. Serbina, M.R. Calin, Optoelectron. Adv. Mater. – Rapid Commun. **5**(3), 273 (2011).
[5] S. Vlase, H. Teodorescu-Draghicescu, D.L. Motoc, M. L. Scutaru, L. Serbina, M.R. Calin, Optoelectron. Adv. Mater. – Rapid Commun. **5**(4), 419 (2011).
[6] S. Vlase, H. Teodorescu-Draghicescu, M. R. Calin, L. Serbina, Optoelectron. Adv. Mater. – Rapid Comm. **5**(4), 424 (2011).
[7] H. Teodorescu-Draghicescu, A. Stanciu, S. Vlase, L. Scutaru, M.R. Calin, L. Serbina, Optoelectron. Adv. Mater. – Rapid Commun. **5**(7), 782 (2011).
[8] R. Purcarea, D. Luca Motoc, M. L. Scutaru, Optoelectron. Adv. Mater. – Rapid Commun. **6**(1-2), 214 (2012).
[9] S. Vlase, H. Teodorescu-Draghicescu, M.R. Calin, M.L. Scutaru, J. Optoelectron. Adv. Mater., **14**(7-8), 658 (2012).
[10] H. Teodorescu-Draghicescu, M.L. Scutaru, D. Rosu, M. R. Calin, P. Grigore, J. Optoelectron. Adv. Mater., **15**(3-4), 199 (2013).
[11] A. Modrea, S. Vlase, H. Teodorescu-Draghicescu, M. Mihalcica, M.R. Calin, C. Astalos, Optoelectron. Adv. Mater. – Rapid Comm. **7**(5-6), 452 (2013).
[12] S. Vlase, R. Purcarea, H. Teodorescu-Draghicescu, M. R. Calin, I. Szava, M. Mihalcica, Optoelectron. Adv. Mater. – Rapid Commun. **7**(7-8), 569 (2013).
[13] J. Wiedemann, Leichtbau. Band 1: Elemente, Springer, (1986).

*Corresponding author: svlase@yahoo.com